molecular pharmaceutics

articles

FTIR Studies on Differential Intermolecular Association in Crystalline and Amorphous States of Structurally Related Non-Steroidal Anti-Inflammatory Drugs

Aditya M. Kaushal,[†] Asit K. Chakraborti,[‡] and Arvind K. Bansal*[,†]

Department of Pharmaceutical Technology (Formulations), and Department of Medicinal Chemistry, National Institute of Pharmaceutical Education and Research, Sector 67, SAS Nagar, Punjab, 160 062, India

Received July 21, 2008; Revised Manuscript Received September 12, 2008; Accepted September 29, 2008

Abstract: Information on molecular interactions critically impacts the physical stability and "stabilization" strategy for the amorphous state of pharmaceuticals. The present study was designed to understand the differences in intermolecular interactions in amorphous and crystalline phases in a series of structurally related compounds- celecoxib (CLB), valdecoxib (VLB), rofecoxib (RFB), and etoricoxib (ETB). FTIR spectra of the compounds in their crystalline and amorphous phase were obtained. Interaction patterns in respective crystalline states were obtained from single crystal data. The intermolecular interaction patterns varied between the crystalline and amorphous phase of CLB, VLB, and ETB, while no variation was observed for RFB. Comparison of four crystalline phases though revealed significantly variations, the interactions were remarkably similar in the amorphous state, possibly as a result of constraints of crystal packing ceasing to exist. Conversion of crystalline state to amorphous state led to weakening of some interactions while others got strengthened. The differences in intermolecular interactions could successfully explain the differences in thermodynamic properties studied previously (Kaushal, A. M.; Bansal, A. K. Thermodynamic behavior of glassy state of structurally related compounds. *Eur. J. Pharm. Biopharm.* **2008**, *69*, 1067−1076.).

Keywords: Infrared spectroscopy; crystalline; amorphous; hydrogen bonding; molecular interactions

Introduction

The importance of amorphous forms for pharmaceuticals has long been realized.[1−5] Apart from affording a higher solubility (and possibly higher bioavailability) for difficult to deliver drugs, an amorphous form can also improve processability. The considerable quantum of research in the field has, however, not translated into practical benefits, and the reach of these systems to the market has been abysmal. This failure can at least in part be attributed to an insufficient understanding of these systems at the molecular level. An understanding of the molecular interactions in the amorphous phase and its differences from that of the crystalline counterparts can potentially help in controlling the behavior of these systems at the macroscopic level.

Intermolecular interactions in the amorphous solids can directly affect their molecular mobility. The latter is recog-

* Author to whom correspondence should be addressed. Mailing address: NIPER, Pharmaceutical Technology (Formulations), Sector 67, Phase X, SAS Nagar, Punjab, 160 062, India. Tel: +91-172-2214682-87. Fax: +91-172-2214692. E-mail: akbansal@niper.ac.in, bansalarvind@yahoo.com.

[†] Department of Pharmaceutical Technology (Formulations).

[‡] Department of Medicinal Chemistry.

(1) Angell, C. A. The old problems of glass and the glass transition, and the many new twists. *Proc. Natl. Acad. Sci. U.S.A.* **1995**, *92*, 6675–6682.

(2) Craig, D. Q. M.; Royall, P. G.; Kett, V. L.; Hopton, M. L. The relevance of the amorphous state to pharmaceutical dosage forms: Glassy drugs and freeze dried systems. *Int. J. Pharm.* **1999**, *179*, 179–207.

(3) Hancock, B. C. Disordered drug delivery: destiny, dynamics and the Deborah number. *J Pharm. Pharmacol.* **2002**, *54*, 737–746.

(4) Hancock, B. C.; Zografi, G. Characteristics and significance of the amorphous state in pharmaceutical systems. *J. Pharm. Sci.* **1997**, *86*, 1–12.

(5) Kaushal, A. M.; Gupta, P.; Bansal, A. K. Amorphous Drug Delivery Systems: Molecular Aspects, Design and Performance. *Crit. Rev. Ther. Drug Carrier Syst.* **2004**, *21*, 133–193.

10.1021/mp800098d CCC: $40.75
Published on Web 10/21/2008

nized as one of the most important determinants of the behavior of amorphous systems.[6] For example, it is known that inorganic silica that exhibits network forming ability by way of intermolecular associations exhibits a "strong" behavior as opposed to non-network forming "fragile" liquids.[1] Moreover, intermolecular associations (especially hydrogen bonding) have been reported to influence T_g.[7] Properties of amorphous forms such as enthalpy relaxation, structural relaxation, devitrification, fragility, glass transition, entropy, free energy and aqueous solubility are all a reflection of the molecular level properties of amorphous solids. An understanding of the intermolecular interactions in the amorphous state also allows selection of "stabilizers" based on the presence of complementary functional groups. Numerous studies on intermolecular interactions in amorphous solid dispersions have been published;[8−10] however, investigations on differential molecular interactions in crystalline and amorphous forms have been rare.[11]

Molecular arrangement in a crystalline solid can be studied through single crystal XRD or neutron scattering studies.[12] However, the amorphous counterparts being devoid of any lattice arrangement[13] are not amenable for investigation by these techniques. This calls for alternative approaches to study the molecular associations in amorphous phase, one of which is infrared spectroscopy. Infrared spectroscopy is based on the principle of bond strength and allows study of intermolecular interactions, involving one or more chemical moieties that lead to change in dipole as a result of unassociated or differently associated chemical conformation. The hydrogen bond is the strongest of all the intermolecular interactions and consequently leads to most discernible changes in FTIR spectra. Besides classical hydrogen bonds, other types of intermolecular interactions such as hydrogen bonds involving weaker groups like C−H group or those with a π cloud, $\pi-\pi$, van der Waals interactions, and other types of electrostatic attractions and repulsions play important roles in the packing arrangement of crystals. A molecular arrangement that satisfies steric constraints and maximizes the density is most likely to be found in crystalline solids.[14] These interactions are likely to differ in the amorphous solids where constraints of crystal packing cease to exist and changes in the strength of molecular interactions or the formation of new interactions may result.

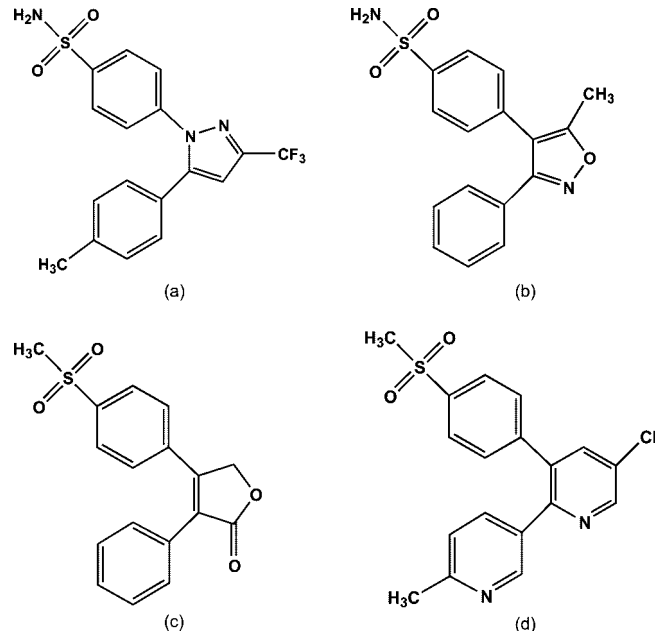

Figure 1. Structure of the four model compounds selected for study: CLB (a), VLB (b), RFB (c), and ETB (d).

The purpose of the present investigation was to gain an understanding of the molecular level interactions in amorphous and crystalline phases of a series of structurally related drugs viz. celecoxib (CLB), valdecoxib (VLB), rofecoxib (RFB), and etoricoxib (ETB) (Figure 1). These drugs belong to an important class of therapeutic agents, non-steroidal anti-inflammatory agents and act as selective COX-2 inhibitors. In an earlier work,[15] we have shown that these four structurally related compounds showed distinct differences in the thermodynamic properties of enthalpy, entropy, free energy and fragility, leading to differences in physical stability. The objective of this work therefore was to investigate the molecular level reasons for the differences seen on thermodynamic and macroscopic basis. The study is based on the hypothesis that the intermolecular interactions/association existing in the crystalline and amorphous states can significantly differ as dictated by the chemical structure and the altered spatial arrangement of molecules in the two phases.

(6) Hancock, B. C.; Shamblin, S. L. Molecular mobility of amorphous pharmaceuticals determined using differential scanning calorimetry. *Thermochim. Acta* **2001**, *380*, 95–107.
(7) Taylor, L. S.; Zografi, G. Sugar-polymer hydrogen bond interactions in lyophilized amorphous mixtures. *J. Pharm. Sci.* **1998**, *87*, 1615–1621.
(8) Doherty, C.; York, P. Evidence for solid- and liquid-state interactions in a furosemide-polyvinylpyrrolidone solid dispersion. *J. Pharm. Sci.* **1987**, *76*, 731–737.
(9) Tajber, L.; Corrigan, O. I.; Healy, A. M. Physicochemical evaluation of PVP-thiazide diuretic interactions in co-spray-dried composites—analysis of glass transition composition relationships. *Eur. J. Pharm. Sci.* **2005**, *24*, 553–563.
(10) Taylor, L. S.; Zografi, G. Spectroscopic characterization of interactions between PVP and indomethacin in amorphous molecular dispersions. *Pharm. Res.* **1997**, *14*, 1691–1698.
(11) Tang, X. C.; Pikal, M. J.; Taylor, L. S. A spectroscopic investigation of hydrogen bond patterns in crystalline and amorphous phases in dihydropyridine calcium channel blockers. *Pharm. Res.* **2002**, *19*, 477–483.
(12) Tromp, R.; Parker, R.; Ring, S. A neutron scattering study of the structure of amorphous glucose. *J. Chem. Phys.* **1997**, *107*, 6038–6049.
(13) Yu, L. Amorphous pharmaceutical solids: preparation, characterization and stabilization. *Adv. Drug Delivery Rev.* **2001**, *48*, 27–42.
(14) Brock, C. P.; Dunitz, J. D. Towards a grammar of crystal packing. *Chem. Mater.* **1994**, *6*, 1118–1127.
(15) Kaushal, A. M.; Bansal, A. K. Thermodynamic behavior of glassy state of structurally related compounds. *Eur. J. Pharm. Biopharm.* **2008**, *69*, 1067–1076.

Experimental Section

Materials. CLB (Unichem Laboratories, Mumbai), VLB (Aarti Drugs, Mumbai), RFB (Ranbaxy Research Laboratories, Gurgaon), and ETB (Aarti Drugs, Mumbai) were used as received, and each had an assay value of >99.9%.

Preparation of Amorphous Forms. Amorphous forms of CLB, VLB, RFB, and ETB were prepared by quenching the drug melts in a differential scanning calorimeter. A small quantity (3−5 mg) of crystalline drug was heated in a pinholed aluminum pan to a temperature 20 °C above the respective melting points, held for 1 min, and then cooled to 25 °C at a rate of 20 °C/min. A rerun of the samples showed glass transitions without any crystallization or melting, there by confirming the formation of amorphous forms. The high-performance liquid chromatography assay of the amorphous samples established that no degradation occurred during the preparation of amorphous forms. Samples were analyzed immediately after preparation, and care was taken to avoid exposure to atmospheric humidity by performing experiments in controlled humidity environment (15 ± 5% RH).

FT Infrared Spectroscopy. The FTIR transmission spectra of the crystalline and the amorphous forms of all four drugs were recorded on a Perkin-Elmer spectrometer (Spectrum One, Perkin-Elmer, Buckinghamshire, U.K.), equipped with spectrum v3.02 software, by the conventional KBr pellet method. Use of an attenuated total reflectance (ATR) accessory confirmed that the peak positions were unchanged due to pellet formation procedure. Each pellet was scanned 32 times at a resolution of 2 cm^{-1}. Band positions for various groups were assigned based on the previous reports in literature.[16,17] Differences in the spectra with respect to band positions (in wavenumbers, cm^{-1}) and band intensities (in percentage transmission) in crystalline and amorphous phases of the drugs were determined.

Single Crystal Data Analysis. Single crystal data[18−21] of the crystalline forms of drugs were used to construct the unit cells of the respective compounds, using the Mercury program (version 1.4.2, Cambridge Crystallographic Data Centre, Cambridge, U.K.). The information on hydrogen bonding patterns was utilized to facilitate interpretation of any IR band shifts observed in case of amorphous samples. Conditions for hydrogen-bond display were defined in the software as an actual distance of less than 4.0 Å. Both the conditions of hydrogen atom being required to be present and not required were used, and all possible donor and acceptor atom types were allowed. The distance H···A, and X—H···A were obtained. The X—H···A angle was set at >90°. The hydrogen bonds were considered to be of moderate strength if the H···A distance was between 1.5 and 2.2 Å and X—H···A distance was 2.5 to 3.2 Å. A weak hydrogen bond was described by values of 2.2 to 3.2 Å and 3.2 to 4.0 Å, respectively.[22]

Results and Discussion

The drugs included in the study have both sufficient degrees of similarity as well as dissimilarity in their chemical structures. The common structural features are that (i) these belong to a tricyclic system with a central heterocyclic ring and having a 1,2-diaryl substitution, and (ii) one of the aryl moieties has a sulfonamide group in case of CLB and VLB, whereas a methyl sulfone group is present in the case of RFB and ETB. The significant structural variations include (i) the presence of a CF_3 group on the central heterocyclic ring in CLB, (ii) an α,β-unsaturated lactone moiety representing the central heterocyclic ring in RFB, (iii) a chlorine substituent in the central heterocyclic ring of ETB, and (iv) one of the aryl substitution attached to the central ring in ETB is 2-methyl pyridine.

Both CLB and VLB possess a sulfonamide group, the hydrogen atoms of which can be available for hydrogen bonding. In contrast, RFB and ETB apparently do not have any hydrogen-bond donor groups. The proton acceptors available for hydrogen bonding in the four compounds under study are (i) the two oxygen atoms of the sulfonamide/sulfone group in these molecules, (ii) the fluorine atoms of the CF_3 group and the nitrogen atom in central hetrocyclic ring in the case of CLB, (iii) carbonyl oxygen atom of the lactone ring in RFB, (iv) the oxygen and nitrogen atoms of the central hetrocyclic ring in VLB, and (v) the chlorine atom attached to the central pyridine ring in case of ETB.

Spectroscopic Studies of Hydrogen Bonding. The formation of a hydrogen bond leads to changes in the bond strengths of both the acceptor and donor groups.[23] The frequency of the donor X—H stretching vibration is more sensitive to the formation of hydrogen bond and is easy to identify. The common changes in the FTIR spectra include (i) red shift in absorption band, (ii) band broadening, and (iii) band intensification. The red shift to downward wavenumbers is proportional to the strength of the hydrogen bond and is caused by the lengthening of the X—H bond due to hydrogen bond formation. Furthermore, an approximate relationship between the hydrogen-bond distance (determined from crystallographic data) and the peak position of the X—H

(16) Pavia, D.; Lampman, G.; Kriz, G. *Introduction to spectroscopy*, 3rd ed.; Harcourt College Publishers: Fort Worth, 2000.
(17) Socrates, G. *Infrared characteristic group frequencies-Tables and charts*, 2nd ed.; John Wiley and Sons, Inc.: New York, 1994.
(18) Dev, R. V.; Rekha, K. S.; Vyas, K.; Mohanti, S. B.; Kumar, P. R.; Reddy, G. O. Celecoxib, a COX-II inhibitor. *Acta Crystallogr.* **1999**, *C55*, IUC9900161.
(19) Rekha, K. S.; Vyas, K.; Raju, C. M. H.; Chandrashekar, B.; Reddy, G. O. Viox, a COX-II inhibitor. *Acta Crystallogr.* **2000**, *C56*, e68.
(20) Savitha, G. Indian Institute of Technology Kanpur, personal communication, 2005.
(21) Sony, S. M. M.; Charles, P.; Ponnuswamy, M. N.; Yathirajan, H. S. Valdecoxib, a non-steroidal anti-inflammatory drug. *Acta Crystallogr.* **2005**, *E61*, o108–o110.
(22) Jeffrey, G. A. *An Introduction to Hydrogen Bonding*; Oxford University Press: New York, 1997.
(23) Steiner, T. The hydrogen bond in the solid state. *Angew. Chem., Int. Ed.* **2002**, *41*, 48–76.

Table 1. FTIR Band Assignments, Positions, and Intensities for Various Functionalities in CLB, VLB, RFB, and ETB

	CLB				VLB				RFB				ETB			
	crystalline		amorphous		crystalline		amorphous		crystalline		amorphous		crystalline		amorphous	
vibration	pos (cm^{-1})	int (%T)	pos (cm^{-1})	int (% T)	pos (cm^{-1})	int (% T)	pos (cm^{-1})	int (% T)	pos (cm^{-1})	int (% T)	pos (cm^{-1})	int (% T)	pos (cm^{-1})	int (% T)	pos (cm^{-1})	int (% T)
N−H stretch	3341	44.7	3347	4.8	3377	60.5	*a*	*b*								
	3234	35.8	3258	4	3249	51.3	3256	10.5								
N−H bend	1563	21.7	1558	12.4	1544	11.8	1544	22.9								
S = O stretch (asym)	1348	43.8	1331	24.8	1334	47.9	1338	28.4	1309	39.8	1309	20.3	1298	54.6	1310	55.2
S = O stretch (sym)	1164	26.7	1164	44.2	1150	44.8	1164	40.1	1148	38	1147	38.1	1144	37	1152	37
C−F stretch (asym)	1276	57.2	1280	9.7												
C−F stretch (sym)	1230	56.1	1241	33.3												
C = O stretch									1748	59	1748	57.1				
Ar−Cl stretch													1085	23.5	1089	15.3
C−H stretch (of CH_3)	2928	5.5	2928	2.3	2929	4	2929	11.9	2931	10.6	2927	25.1	2964	2	2964	0.7
	2868	2.4	2868	1	2874	1.5	2874	0.7	2956	1.1	2964	0.7	2927	8.9	2924	8.1
									2866	3.6	2866	5.8	2861	1.4	2861	1.6
C−H stretch (of ar ring)	3099	17.5	3069	5.7	3091	6.2	3066	7.8	3019	9.6	3020	10.8	3026	4.4	3020	1.2
													3057	11.2	3040	3.4
													3000	5.1	*a*	*b*

[a] Not sufficiently resolved peak. [b] Reduced intensity; pos, position; int, intensity; ar, aromatic; sym, symmetric; asym, asymmetric.

group has been indicated,[24] whereby a lower peak frequency correlates with a shorter hydrogen bond distance (i.e., stronger hydrogen bond and longer X−H bond). A direct effect of hydrogen bond can also be observed on the acceptor side, due to weakening of the bond, leading to a lowering of stretching vibration.

The bandwidth and integrated band intensities increase strongly upon formation of a hydrogen bond, and have been suggested as more reliable indicators of hydrogen-bond formation than the red shift of stretching frequency.[25] However, this may be truly applicable in the case of systems where the comparisons are made between two crystalline compounds, and a hydrogen bond either exists or is absent. Band width and intensities have little relevance when crystalline and amorphous systems are compared, wherein the latter is expected to exhibit a general nonspecific band broadening and decrease in band intensity. Additionally amorphous systems may involve a weakening or strengthening of hydrogen bonds thus leading to decrease in band intensities, due to the general diffusion and broadening. However, an increase in the band intensity in the amorphous phase (instead of decrease in spite of diffusion) was considered as an indication of strengthening of hydrogen bonding in the amorphous phase.

The FTIR spectra of crystalline and amorphous forms showed noticeable changes, with the latter exhibiting generalized broadening and diffusion of bands that can be attributed to the differences in hydrogen-bonding patterns in the two solid-state forms. This can be attributed to the relative disorder of the molecules in the amorphous form, resulting in a broader distribution of bond lengths and energies with respect to the crystalline counterparts. Table 1 summarizes the various band assignments, their wavenumber positions and their respective intensities, for the four model compounds in their crystalline and amorphous phases.

Celecoxib. CLB has a variety of chemical groups that can potentially hydrogen bond with groups of another molecule. In an earlier report,[26] we had utilized FTIR and molecular modeling to study the molecular interactions in crystalline and amorphous CLB. In the present study, interactions in CLB have been studied in greater detail to facilitate comparisons with other three molecules. In the solid state, sulfonamides have strong bands due to their N−H stretching vibrations in the region 3390−3245 cm^{-1}.[17] Moreover, hydrogen bonds produced by N−H moieties can shift the band positions toward lower wavenumbers. The SO_2 group, due to its strong electron withdrawing nature, is able to polarize the nitrogen atom positively, which in turn eases the release of protons.[27] For the very same reason, the amido N loses its electron donating capability due to delocalization of its electrons over the neighboring O atoms.[28]

Crystalline CLB showed a doublet at 3341 cm^{-1} and 3234 cm^{-1} for N−H stretching vibrations (Figure 2a). The low position of this N−H band *per se* was indicative of its participation in hydrogen bonding. The doublet was shifted

(24) Nakamoto, K.; Margoshes, M.; Rundle, R. E. Stretching frequencies as a function of distances in hydrogen bonds. *J. Am. Chem. Soc.* **1955**, *77*, 6480–6486.

(25) Lutz, B.; Jacob, J. van der Maas, Vibrational spectroscopic characteristics of =C---H. . O and N---H. . π interaction in crystalline N-(2,6-dimethylphenyl)-5-methylisoxazole-3-carboxamide. *J. Vib. Specrosc.* **1996**, *12*, 197–206.

(26) Gupta, P.; Thilagavathi, R.; Chakraborti, A. K.; Bansal, A. K. Differential molecular interactions between the crystalline and the amorphous phases of celecoxib. *J Pharm Pharmacol.* **2005**, *57*, 1271–1278.

(27) Patai, S.; Rappaport, Z. *The chemistry of sulfonic acids, esters and their derivatives*; John Wiley and Sons: Chichester, 1991.

(28) Adsmond, D. A.; Grant, D. J. W. Hydrogen bonding in sulfonamides. *J. Pharm. Sci.* **2001**, *90*, 2058–2077.

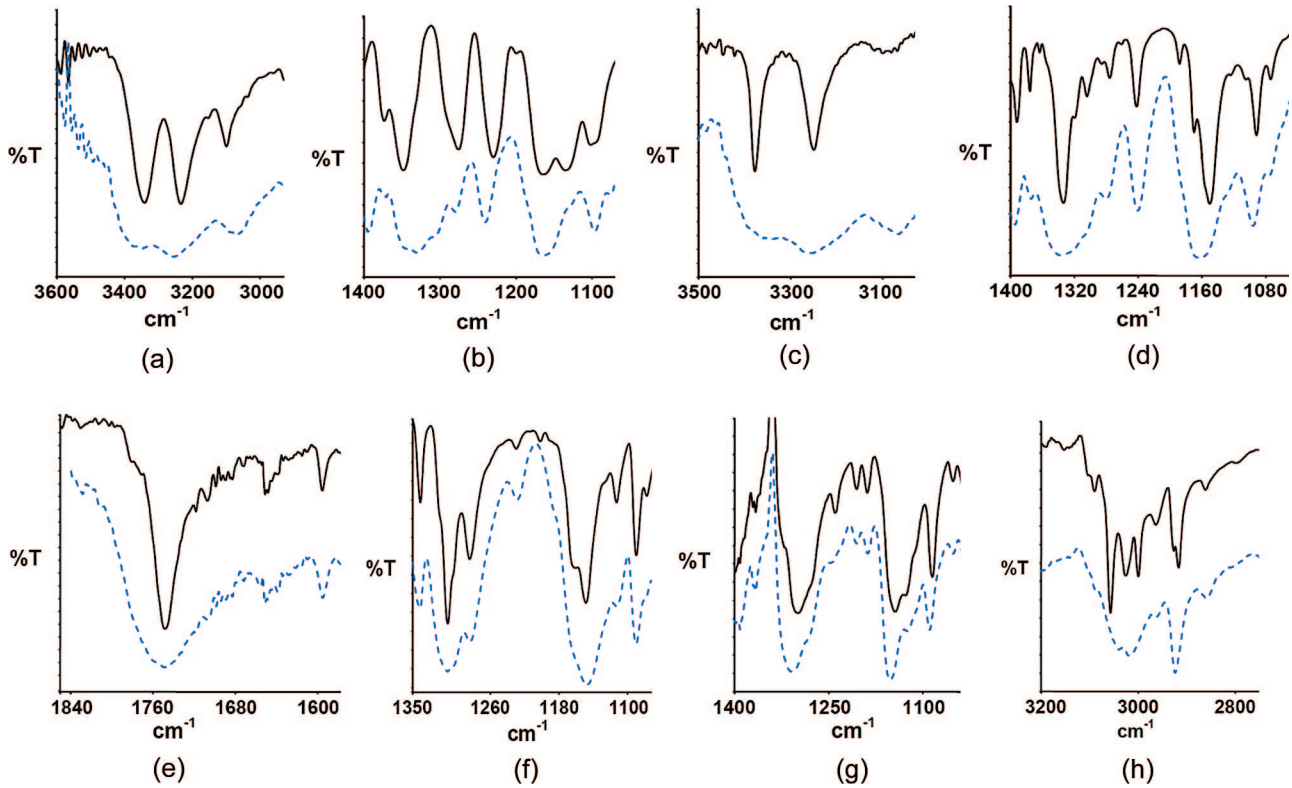

Figure 2. FTIR stretching regions for CLB NH_2 (a); CLB S═O and C−F (b); VLB NH_2 (c); VLB S═O (d); RFB C═O (e); RFB S═O (f); ETB S═O (g); and ETB C−H (h) regions. The solid line represents the spectrum of the crystalline form, and the dashed spectrum is for the amorphous form.

upward to values of 3347 cm^{-1} and 3258 cm^{-1} in the amorphous form. The N−H bending vibration on the other hand showed a downward shift from 1563 cm^{-1} in crystalline form to 1558 cm^{-1} in the amorphous form. Both the lowering of stretching frequency and increase of bending frequency are associated with hydrogen bonding.[17] The above observations indicate a strengthening of the N−H bond in the amorphous form due to weakening or a disruption of hydrogen bonding in the amorphous CLB, as compared to the crystalline sample.

The S═O vibrations appeared as 1348 cm^{-1} (asym) and 1164 cm^{-1} (sym). In amorphous CLB, the asymmetric stretch shifted to a value of 1331 cm^{-1}. The symmetric stretch, although it did not show any shift in peak position, exhibited an increase in intensity in the amorphous phase (Figure 2b). This indicated that the oxygen atom of the sulfonamide group in the crystalline CLB was involved in a weaker interaction, which changes to a more strongly bonded state in the amorphous form. The strengthening of hydrogen bonds in the amorphous state, although less commonly encountered, has been reported previously.[11] The third potential hydrogen-bond forming group in CLB is the CF_3 group that showed bands at 1230 cm^{-1} (asym) and 1276 cm^{-1} (sym) in the crystalline form, which changed to 1241 cm^{-1} and 1280 cm^{-1}, respectively, in the amorphous phase (Figure 2b). This indicated that CF_3, similar to the N−H moiety, was interacting much more strongly in the crystalline form than in the amorphous phase.

In addition to the above groups capable of classical hydrogen-bond formation, the stretching frequencies of the CH_3 group attached to the benzene ring and the C−H (aromatic) were investigated. The bands corresponding to the C−H stretch of methyl group appeared at 2928 cm^{-1} (asym) and 2868 cm^{-1} (sym), in the case of both the states. The C−H stretch for aromatic ring appeared at 3099 cm^{-1} in the crystalline form, and shifted to 3069 cm^{-1} in the amorphous phase, probably due to greater conformational flexibility in the amorphous state, thus allowing increased interaction of the aromatic C−H with other functionalities in the molecule, resulting in a decrease in the stretching frequency.

The single crystal data analysis of CLB[18] showed the presence of five hydrogen bonds that fulfilled the criteria of maximum distance and minimum angle. These are listed in Table 2, indicating the groups associated, H···A distance, X···H−A distance, and X···H−A angle. Hydrogen bonds were found to exist between the amido hydrogens of one molecule with the S═O of other molecule; amido hydrogen and N of pyrazole ring, and between amido hydrogen and two fluorine atoms. The hydrogen-bond distances indicate that the N−H···F hydrogen bond was the weakest of all though F is the most electronegative atom. This indicates the role of factors other than hydrogen bonding (such as maximization of density)[14] in determining the packing pattern of molecules in a unit cell.

Table 2. Hydrogen-Bond Patterns and Properties for the Compounds in Their Crystalline State Obtained from Single Crystal Data[a]

			distance (Å)		angle (deg)
compound	acceptor atom	donor hydrogen	H···A	X−H···A	X−H···A
CLB	O^2	$H^{13}N^3$	2.085	2.952	172.4
	N^1	$H^{14}N^3$	2.235	3.087	166.9
	F^2	$H^{13}N^3$	2.909	3.170	99.4
	F^2	$H^{14}N^3$	2.983	3.855	94.4
	F^3	$H^{14}N^3$	3.182	3.441	100.0
VLB	O^{13}	$H^{15}N^{15}$	2.121	3.009	168.8
	O^{14}	$H^{15}N^{15}$	3.218	3.825	126.8
ETB	O^2	$H^{35}C^{35}B$	2.530	3.462	163.8
	O^2	$H^{19}C^{19}$	2.430	3.329	162.6
	Cl^4	H^9C^9	2.823	3.580	139.2

[a] Numerical superscripts as described in single crystal data of the respective compounds differentiate atoms of the same type in a molecular structure, e.g. H^{13} and H^{14} correspond to two Hs in NH_2 in CLB.

Valdecoxib. In crystalline VLB, the N−H stretching vibration appeared as a doublet at 3377 cm^{-1} and 3249 cm^{-1}. In the amorphous state, these bands became highly diffused, with the 3377 cm^{-1} peak appearing as a shoulder to the peak at 3256 cm^{-1} that shifted from its position of 3249 cm^{-1} in the crystalline state (Figure 2c). As in the case of CLB, this indicated a weaker bonding in amorphous phase, though the shift of band position was lower than in case of CLB. The SO_2 group appeared at 1150 cm^{-1} (sym) and 1334 cm^{-1} (asym) (Figure 2d). These were shifted to higher wavenumbers in the amorphous form, with change to 1164 cm^{-1} and 1338 cm^{-1}, respectively. Thereby, it can be inferred that the hydrogen-bonding association involving the S═O group is stronger in the crystalline state. These results were contrary to those encountered for CLB, where an increase in the interactions involving the S═O group was indicated for the CLB amorphous phase. The concomitant increase in the stretching frequencies of both N−H and S═O groups is indicative of breakage of interactions between these two groups.

The bands corresponding to the C−H stretch of methyl substituent on the isoxazole ring appeared at 2929 cm^{-1} (asym) and at 2874 cm^{-1} (sym), and remained unchanged in the amorphous phase, signifying the absence of any interaction involving the methyl group. Similar to CLB, the C−H stretch for aromatic ring shifts from 3091 cm^{-1} in the crystalline form to 3066 cm^{-1} in the amorphous phase. The shift to lower wavenumber can be thought to result from stronger association of the aromatic rings in the amorphous phase. The band intensity also increased in the amorphous sample, thus complementing the band shift results. As with CLB, the stronger associations for aromatic C−H in VLB in the amorphous phase are indicative of newer associations with other functionalities upon randomization of molecular arrangement in the amorphous phase. The C−H in itself is not a preferred hydrogen-bond donor and is likely to be largely ignored in crystal packing.

The single crystal data of VLB[21] showed the presence of hydrogen bonding between one of the amido nitrogens with the two O's of the sulfonamide moiety of another molecule, thus substantiating the FTIR results, where a strong interaction was apparent in the crystalline phase. From the FTIR observation, it is likely that these bonds are broken/diminished in the amorphous phase.

Comparison between CLB and VLB. Both CLB and VLB possess a sulfonamide moiety, and a comparison of the SO_2 and N−H stretching frequencies was made to bring out the differences in the two compounds in their crystalline and amorphous states. The S═O stretching (both symmetric and asymmetric) in the case of crystalline VLB appeared at lower wavenumbers when compared to crystalline CLB. This was indicative of a greater extent of intermolecular hydrogen bonding involving the S═O group of one molecule with the N−H of other molecule in VLB. To substantiate this observation, we compared the spatial disposition of the molecules in the unit cell crystal structure of CLB and VLB. In the case of CLB, only two molecules were accommodated in the unit cell and only one oxygen atom of the SO_2 group was involved in hydrogen bonding with N−H of other molecule. Even taking into consideration the unit cell in tandem, no hydrogen-bonding interaction could be observed for the second O atom of SO_2 group (the measured distance of this O and another probable hydrogen of N−H was 4.277 Å, which does not provide for a plausible hydrogen-bonding interaction).[22] In the case of VLB, eight molecules were accommodated in one unit cell and both the O atoms of a particular SO_2 moiety were involved in intermolecular hydrogen bonding involving the N−H group of another molecule, with the corresponding distances of 2.121 Å and 3.218 Å. Thus the average hydrogen-bonding interaction was more in the crystalline VLB than that in crystalline CLB, thereby explaining the FTIR observations.

N−H stretching frequency peaks were sharper, narrower and higher in wavenumbers for crystalline VLB as compared to that of crystalline CLB, thus indicating a lower extent of intermolecular hydrogen bonding involving the N−H group. This might appear counterintuitive taking into consideration the hydrogen bond involving the S═O and N−H groups, since this type of hydrogen bond is more prominent in VLB. The reason for this behavior can be found if one considers the global type (other type) of hydrogen-bonding interaction involving the N−H group, rather than concentrating on the localized hydrogen bonds involving the S═O and the N−H.

From the crystal structures of the two compounds, it is seen that in the case of CLB one hydrogen atom of the SO_2NH_2 group is involved in hydrogen-bond formation with the S═O group and the F atom of the CF_3 group of two different molecules (Figure 3a). This hydrogen-bonded interaction leads to an intermolecular association, while the second N−H hydrogen is hydrogen bonded with the N atom of the central heterocyclic ring of another molecule and with two F atoms of the CF_3 group of the same molecule (Figure 3b) which in turn folds back (bimolecular ring)[28] to project its sulfonamide moiety such that one of the hydrogen atoms

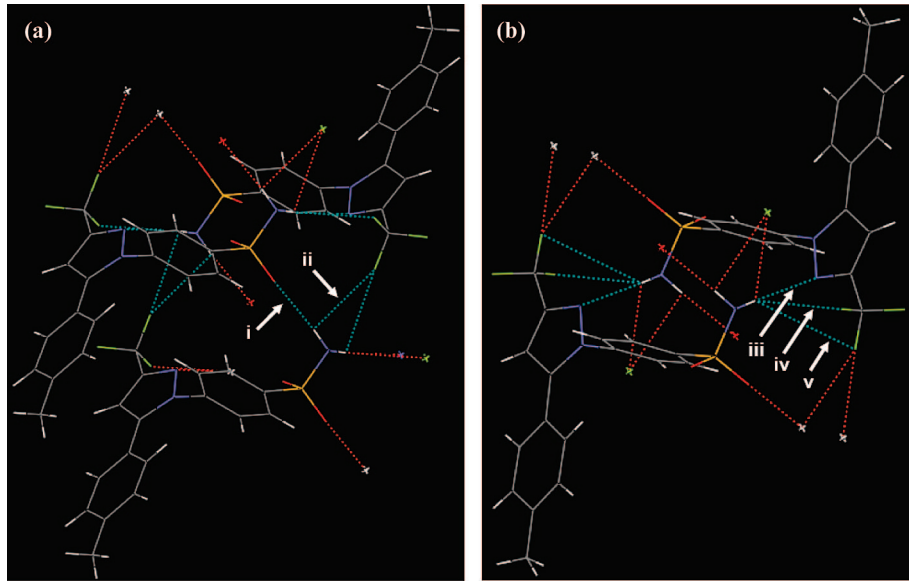

Figure 3. Hydrogen-bonding pattern for CLB in its crystalline state. One of the two NH_2 hydrogens is hydrogen bonded to S═O (i), and F of the CF_3 group (ii), of two different molecules (a). The other hydrogen is hydrogen bonded to pyrazole N (iii), and two F atoms of CF_3 group (iv and v) of the same molecule (b). The figure was drawn using the Mercury program (version 1.4.2) and the cif file in ref 18.

of the SO_2NH_2 group forms a hydrogen bond with two F atoms of the CF_3 group and the N atom of the central ring of the first molecule. The well-organized five-membered transition state/structure arising out of this hydrogen-bond framework makes this hydrogen bond very effective. However, in the case of VLB, only one H of the SO_2NH_2 group is engaged in hydrogen bonding with the S═O group of another molecule and the second hydrogen of nitrogen was not involved in any association. Thus the average hydrogen-bond interaction involving the N−H atom is more in the case of crystalline CLB than that in crystalline VLB, and this accounts for the observed differences in the FTIR spectra.

Another interesting observation relates to the comparison of band positions for N−H and S═O groups in the amorphous phases of the two molecules. One of the N−H stretching vibrations appeared almost at similar position in amorphous CLB and amorphous VLB (3257 cm^{-1} and 3256 cm^{-1}, respectively). Similarly, the symmetric stretching vibration for SO_2 group appeared at 1164 cm^{-1} in both CLB and VLB. The above observations point to the fact that the strength of bonds is almost similar in the structurally related molecules in their amorphous phases. In the crystalline state, the constraints of crystal packing dictate the similar groups present in different molecules to have a different intermolecular interaction patterns; however in the amorphous phase where such constraints cease to exist, these groups exhibit similar bond strengths reflected in near similar stretching frequencies. Similar observations were made by Tang et al.[11] for the amorphous state of dihydropiridine calcium channel blockers.

Rofecoxib. RFB has a lactone carbonyl and SO_2 group that can potentially act as hydrogen-bond acceptors; however, no hydrogen-bond donors are present. Crystalline RFB showed a carbonyl C═O stretch of the lactone ring at 1748 cm^{-1}. This peak showed a general broadening although there was no change in the peak position (Figure 2e), thereby indicating that this group was not involved in any discernible association in crystalline or amorphous phase. The SO_2 stretching vibrations appeared at 1148 cm^{-1} and 1309 cm^{-1} for symmetric and asymmetric stretch, respectively (Figure 2f). Neither of these bands exhibited any change except the general broadening, indicating the absence of intermolecular associations involving the SO_2 groups. The C−H stretch of the methyl in the SO_2 group and the C−H stretch of the aromatic ring also did not show any appreciable change, thereby ruling out the possibility of any type of interactions in either phase of RFB.

The single crystal data for RFB[19] shows that there are only weak van der Waals interactions between molecules in the unit cell of crystalline RFB. This is concordant with the fact that the RFB structure has no hydrogen bond donors in the molecule and therefore there exists no possibility of hydrogen bonding even with a strong carbonyl acceptor. This explains the lack of changes observed for either the C═O stretch or the S═O stretching frequencies in crystalline and amorphous RFB.

Etoricoxib. Similar to RFB, ETB chemical structure does not have any classical hydrogen-bond donors, though hydrogen-bond acceptors—SO_2 group and the N atom—are present. Interestingly, though, substantial differences in the FTIR spectra of the crystalline and amorphous ETB were observed. The SO_2 stretching vibrations in crystalline form, appeared at 1144 cm^{-1} and 1298 cm^{-1} for symmetric and asymmetric stretch, respectively (Figure 2g). Both of these bands showed an appreciable increase of 8 and 12 cm^{-1} in

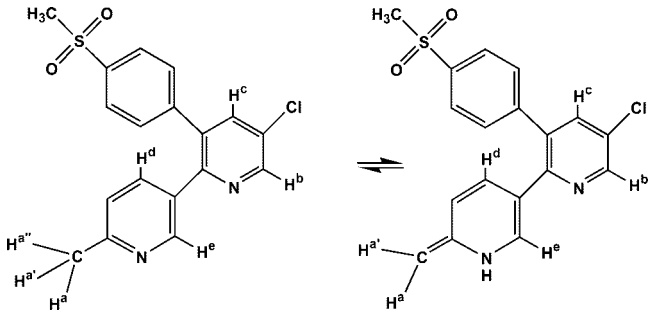

Figure 4. Chemical structure of ETB indicating the hydrogen atoms capable of undergoing nonconventional hydrogen-bonding interaction. The tautomeric structure involving the pyridine ring having a methyl substituent is also shown.

wavenumber to values of 1152 cm^{-1} and 1310 cm^{-1}, respectively.

The changes observed for ETB can be reconciled if other types of hydrogen bonds are considered in the absence of conventional hydrogen bonds. Since the methyl moiety of the SO_2 group is not capable of forming a hydrogen bond (as shown by the inability to do so in the case of RFB), it is the methyl group at the pyridine ring that is likely to be involved in the hydrogen bonding. The hydrogen atoms that are capable of taking part in nonconventional hydrogen bond formation are (i) hydrogen atom of the CH_3 group attached to the pyridine ring and (ii) hydrogen atoms at ortho and para positions with respect to the nitrogen atom of the pyridine ring. The hydrogen atoms of the methyl group attached to the pyridine nucleus are of significantly higher acidity than the hydrogen atom attached to a benzenoid nucleus. Due to the strong electromeric effect of a C═N bond, the ortho and para hydrogens of a pyridine nucleus become capable of hydrogen-bond formation. These hydrogens that are capable of undergoing nonconventional hydrogen-bonding interaction along with the tautomeric structure involving the pyridine ring are also shown in Figure 4. The FTIR observation was further substantiated by the interatomic distance of 2.530 Å, observed between one of the H on CH_3 of pyridine (H^a) and O of the sulfone moiety in the single crystal of ETB,[20] thereby indicating possible interaction between the two centers. The hydrogen-bonding interaction of the pyridine methyl hydrogen of one molecule with the sulfone oxygen atom of another molecule leads to an intermolecular ring structure involving two molecules. Further, the hydrogen atom (H^b) flanked by the nitrogen and chlorine atoms in the central pyridine ring becomes significantly polar and is found to be within the hydrogen-bond distance (2.430 Å) of the S═O group of another molecule leading to the formation a hydrogen bond. The C-4 hydrogen of the central pyridine ring (H^c) was located in close proximity (2.448 Å) with the S═O moiety of another molecule. This hydrogen bond formation between the S═O and the hydrogen atom of the central pyridine ring may further account for the lower wavenumber of the SO_2 group in the crystalline form. Bands representing the C−H stretching frequency (Figure 2h) also showed significant changes substantiating the reasoning of association between the S═O and C−H groups.

Another prominent change in the FTIR spectra of ETB related to the change in Ar−Cl stretching frequency from 1084 cm^{-1} in crystalline ETB to 1089 cm^{-1} in amorphous ETB. This may be due to some hydrogen-bond interaction involving the Cl atom in the crystalline state. In this case, the distance between the Cl atom and C-4 hydrogen in the methyl substituted pyridine ring (H^d) of another molecule, in single crystal for ETB, was found to be 2.823 Å, which indicated the possibility of interaction between these two groups. Although the H^e hydrogen of the methyl substituted pyridine ring also possesses polar character (due to the adjacent N atom), in the crystalline structure it could not be located within a reasonable distance of any hydrogen-bond acceptor, so as to get involved in hydrogen bonding.

The hydrogen-bond properties of C−H···O bonds have been a matter of continuous debate.[29,30] However, it is now recognized that the donor potential of weakly polarized C−H group may be responsible for its hydrogen-bonding ability. The difference in the hydrogen-bonding capability of C−H bond as against van der Waals interactions lies in its directionality.[31] There is no doubt that C−H···O interactions are formed only as a last resort if the stronger hydrogen bonds are lacking, but if they form, C−H donors actually take the role and functions of O−H or N−H and may even determine crystal packing arrangement.[30]

Comparison between RFB and ETB. The major similarity in the chemical structure of RFB and ETB relates to the presence of a sulfone group. Comparison of the crystalline forms of the two molecules for the S═O stretching vibration showed that the frequency in RFB is higher than that in ETB. This may be ascribed to the hydrogen-bonded nature of the S═O group in ETB, as opposed to unassociated state in RFB. However, in the amorphous state, the asymmetric stretching frequency of S═O for the two molecules was largely similar. This is in accord with the results obtained for CLB vs VLB which also exhibited comparable stretching frequencies in their amorphous states upon loss of crystal constraints.

Importance of Studying Intermolecular Interactions in Crystalline and Amorphous Phases. Molecular level interactions in crystalline and amorphous states can vary significantly based on the chemical moieties present and the spatial constraints of crystal packing in the crystalline form. The new possibilities for intermolecular interactions that emerge due to amorphization can provide useful information for selection of "stabilizers" for amorphous solid dispersions and lyophilized systems. Since the crystallization from amorphous state involves coming together of molecules to

(29) Desiraju, G. Hydrogen bridges in crystal engineering: interactions without borders. *Acc. Chem. Res.* **1991**, *35*, 565–573.
(30) Steiner, T. Unrolling the hydrogen bond properties of C-H. .O interactions. *Chem. Commun.* **1997**, 727–734.
(31) Steiner, T.; Desiraju, G. Distinction between the weak hydrogen bond and the van der Waals interations. *Chem. Commun.* **1998**, 891–892.

re-form the crystalline intermolecular interactions, an in-depth understanding of these interactions (and how they differ from in amorphous state) is the first step toward prevention of crystallization. Selection of polymers having counter groups in terms of hydrogen bonding holds the key for development of stable amorphous dispersions and lyophilized products. Apart from the generalized antiplasticization effect of polymeric interactions, specific drug−polymer interactions dictate the "stability" of the amorphous dispersions. Studies reported from our laboratory[26,32−34] have shown the role of drug−polymer interactions in enthalpy relaxation, shelf life stability, solubility and resistance to devitrification in dissolution environment. These properties determine the overall behavior of amorphous systems in terms of "stability" and solubility advantage.

As mentioned previously, based on the chemical structure, CLB and VLB were expected to behave similarly as against RFB and ETB, due to the absence of hydrogen-bonding capabilities in the latter two. However, this study provided interesting results, where the behavior of ETB was more akin to CLB and VLB in terms of interaction patterns in the respective crystalline and amorphous phases. In our earlier studies[15] aimed at comprehensive thermodynamic characterization of the amorphous phase of the four molecules, RFB showed distinctly greater thermodynamic fragility, higher Kauzmann temperature, and configurational free energy. In thermodynamic terms, the behavior of ETB was more similar to CLB and VLB than to RFB. It can therefore be emphasized that the differences in the thermodynamic behavior and physical stability of the four molecules in their amorphous states arise from the differences in their interaction patterns at the molecular level. The present study successfully explains the macroscopic and thermodynamic differences based on the differences in molecular level behavior.

Conclusions

Utilizing the techniques of FTIR and single crystal data analysis, it was possible to elucidate the molecular interactions inherent to the crystalline and amorphous phases of four structurally related non-steroidal anti-inflammatory drugs. The intermolecular associations in the amorphous and crystalline states were found to vary in CLB, VLB, and ETB, while RFB showed lack of association capability. The varying strength of association in crystalline drugs indicates the influence of factors other than hydrogen bonding in determining the packing pattern in crystals. In the amorphous state, the strengths of similar moieties in the molecules are grossly similar, indicating that the hydrogen-bond strengths tend to be similar when constraints of crystal packing cease to exist. The study brought out inherent differences in association patterns in crystalline and amorphous phase of drugs that can explain differences in thermodynamic and macroscopic behavior of the studied compounds.

Abbreviations Used

CLB, celecoxib; VLB, valdecoxib; ETB, etoricoxib; RFB, rofecoxib; FTIR, Fourier transform infrared spectroscopy; sym, symmetric stretching; asym, asymmetric stretching.

Acknowledgment. A.M.K. would like to acknowledge center for scientific and industrial research (CSIR), for providing senior research fellowship.

MP800098D

(32) Bansal, S. S.; Kaushal, A. M.; Bansal, A. K. Molecular and Thermodynamic Aspects of Solubility Advantage from Solid Dispersions. *Mol. Pharmaceutics.* **2007**, *4*, 794–802.

(33) Gupta, P.; Chawla, G.; Bansal, A. K. Physical stability and solubility advantage from amorphous celecoxib: The role of thermodynamic quantities and molecular mobility. *Mol. Pharmaceutics* **2004**, *1*, 406–413.

(34) Gupta, P.; Kakumanu, V. K.; Bansal, A. K. Stability and solubility of celecoxib-PVP amorphous dispersions: A molecular perspective. *Pharm. Res.* **2004**, *21*, 1762–1769.